

Observational signatures of dark energy produced in an ancestor vacuum: Forecast for galaxy surveys

Daisuke Yamauchi,^{1,*} Hajime Aoki,^{2,†} Satoshi Iso,^{3,‡} Da-Shin Lee,^{4,§} Yasuhiro Sekino,^{5,¶} and Chen-Pin Yeh^{4,**}

¹*Faculty of Engineering, Kanagawa University, Kanagawa, 221-8686, Japan*

²*Department of Physics, Saga University, Saga 840-8502, Japan*

³*Theory Center, High Energy Accelerator Research Organization (KEK),
and Graduate University for Advanced Studies (SOKENDAI), Ibaraki 305-0801, Japan*

⁴*Department of Physics, National Dong-Hwa University, Hualien 97401, Taiwan, R.O.C.*

⁵*Department of Liberal Arts and Sciences, Faculty of Engineering, Takushoku University, Tokyo 193-0985, Japan*

We study observational consequences of the model for dark energy proposed in [1]. We assume our universe has been created by bubble nucleation, and consider quantum fluctuations of an ultralight scalar field. Residual effects of fluctuations generated in an ancestor vacuum (de Sitter space in which the bubble was formed) is interpreted as dark energy. Its equation of state parameter $w_{\text{DE}}(z)$ has a characteristic form, approaching -1 in the future, but $-1/3$ in the past. A novel feature of our model is that dark energy effectively increases the magnitude of the negative spatial curvature in the evolution of the Hubble parameter, though it does not alter the definition of the angular diameter distance. We perform Fisher analysis and forecast the constraints for our model from future galaxy surveys by Square Kilometre Array and Euclid. Due to degeneracy between dark energy and the spatial curvature, galaxy surveys alone can determine these parameters only for optimistic choices of their values, but combination with other independent observations, such as CMB, will greatly improve the chance of determining them.

Introduction.— It is widely accepted that the expansion of the present universe is accelerating. The first clear evidence for acceleration has been provided by observations of supernovae (SNe) of type Ia [2, 3]. Strong support has been given by the fact that other independent phenomena such as cosmic microwave background (CMB), baryon acoustic oscillation (BAO), etc., consistently suggest cosmic acceleration (see e.g., [4] for a review). The source of the accelerating expansion is attributed to dark energy of unknown origin, which has the equation of state (EoS) parameter $w_{\text{DE}} = p/\rho$ close to -1 , contributing about 68% of the critical density [5, 6]. The next generation observations are expected to determine w_{DE} to a percent level, and also its derivative with respect to the scale factor to a 10 percent level [4].

At a time of great observational developments, an important direction of research would be to construct a theoretically motivated model of dark energy, and have it tested by observations. There are models which describe dark energy (see [7] for a review), such as quintessence (scalar field slowly rolling down a potential) and modified gravity, but they typically do not explain its origin. It remains a mystery why its energy density is extremely small compared to the fundamental scale, $\rho_{\text{DE}} \sim 10^{-122} M_{\text{P}}^4$.

In the previous paper [1], five of the present authors proposed a model for dark energy, partially motivated by string landscape. Assuming our universe has been created by bubble nucleation from a metastable de Sitter space (the “ancestor vacuum”), residual effects of quantum fluctuations generated in the ancestor vacuum has been interpreted as the source of dark energy. Its equation of state parameter $w_{\text{DE}}(z)$ has a characteristic form as a function of the redshift z . The purpose of the present

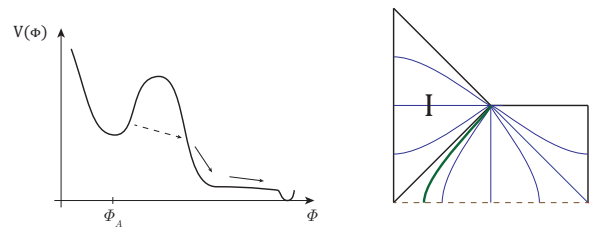


FIG. 1. Left panel: A potential with a metastable de Sitter vacuum. Right panel: Penrose diagram for a bubble nucleated in de Sitter space. The horizontal line at the bottom represents a global slice in de Sitter space at the time of bubble nucleation. The green line is the bubble wall; on its left (right) is the true (ancestor) vacuum. Our universe is an open FLRW universe inside the bubble, represented as Region I.

Letter is to assess the possibility of observational tests of this model. Observations that we consider to be particularly promising are galaxy surveys by Square Kilometre Array (SKA) [8] and Euclid [9], planned to start operating in the early 2020’s. We will perform Fisher analysis and forecast the constraints for our model¹.

The theoretical setup.— We consider bubble nucleation due to quantum tunneling, which occurs e.g., in a potential for a scalar field Φ shown in FIG. 1, left panel. The Hubble parameter of the ancestor vacuum will be de-

¹ Our work focuses on the test of a particular model, and is complementary to the attempts at “model independent” forecasts [10]. The authors of [10] introduce as many parameters as to be considered general, and study emissions from intergalactic medium at $6.3 \lesssim z \lesssim 20$, while we consider a minimal set of parameters and study emissions from galaxies themselves at $z \lesssim 2$.

noted H_A . Our universe is inside the bubble, represented as Region I in FIG. 1, right panel. It should have negative spatial curvature [11]. After bubble nucleation, the ordinary inflation with the Hubble parameter $H_I (\ll H_A)$ is assumed to occur.

We consider a scalar field ϕ which is different from the tunneling field² Φ and has zero expectation value. We assume the field ϕ to have mass m_A before tunneling, and m_0 after tunneling, where m_A and m_0 could be different. The latter is assumed to satisfy $m_0 \lesssim H_0$ where $H_0 \sim 10^{-33}\text{eV}$ is the present Hubble parameter. A candidate for such an ultralight field is one of the axion-like fields, expected to exist in string compactifications³ [16].

In [1], the contribution from the field ϕ to the vacuum expectation value of the energy-momentum tensor $\langle T_{\mu\nu} \rangle$ has been computed, carefully taking into account the effect of the ancestor vacuum. In the free-field approximation, the energy-momentum tensor is quadratic in ϕ , thus $\langle T_{\mu\nu} \rangle$ can be obtained by taking the coincident-point limit of the two-point function $\langle \phi\phi \rangle$ computed by the method developed in⁴ [21–23]. We refer the reader to [1] for details, and give an order-of-magnitude argument here. In the ancestor vacuum, quantum fluctuations give rise to the expectation value of the field-squared $\langle \phi^2 \rangle \sim H_A^4/m_A^2$, as in pure de Sitter space (see e.g., [24]). The field ϕ is almost frozen until now, due to the assumption $m_0 \lesssim H_0$ (and one more condition $\epsilon \ll 1$, to be mentioned below). If so, the energy-momentum tensor is dominated by the mass term, and takes the form of cosmological constant ($w_{\text{DE}} = -1$), with the magnitude

$$\langle T_{\mu\nu} \rangle \sim m_0^2 \langle \phi^2 \rangle g_{\mu\nu} \sim H_A^4 \left(\frac{m_0}{m_A} \right)^2 g_{\mu\nu}. \quad (1)$$

It is not difficult for this to have the same order of magnitude as dark energy, $\rho_{\text{DE}} \sim M_P^2 H_0^2$, once we admit $m_0 \sim H_0$: We just need $m_A/H_A \sim H_A/M_P$, i.e., H_A being the geometric mean of m_A and M_P .

Difference from quintessence.— At the level of the above heuristic argument, it makes no difference whether ϕ is a classical or quantum field. However, fully quantum mechanical analysis in [1] has the following two important differences from the classical case.

First, there is no ambiguity in the initial condition for the field ϕ , unlike in the classical case, in which one has to assign e.g., the axion misalignment angle by hand. Our prediction (1) is unambiguous when H_A , m_A , m_0

are given. This is a virtue of bubble nucleation, which allows us to go past the beginning of the FLRW time and uniquely determine the vacuum state of a quantum field.

Second, the mode of ϕ which gives the dominant contribution at late times is not strictly homogeneous. It is an eigenfunction of the Laplacian on the spatial slice H^3 with a non-zero eigenvalue. There is a peculiar feature of modes on a hyperboloid. Normalizable modes decay exponentially (since the volume grows exponentially) at large distances; they have eigenvalues $\nabla^2 = -(k^2 + 1)$ with real k . However, in an open universe created by bubble nucleation, there is the so-called supercurvature mode [21, 22], which is non-normalizable on H^3 , and has an eigenvalue with imaginary $k = i(1 - \epsilon)$, i.e., $\nabla^2 \sim -2\epsilon$ when $\epsilon \ll 1$. The parameter ϵ is determined by the properties of the ancestor vacuum,

$$\epsilon = c_\epsilon \left(\frac{m_A}{H_A} \right)^2, \quad (2)$$

when $m_A/H_A \ll 1$, with an order-one coefficient c_ϵ which depends on the size of the critical bubble⁵ [1]. The supercurvature mode gives rise to long-range correlations in the open universe, which can be interpreted as the super-horizon fluctuations in the ancestor vacuum, seen from the inside of the bubble.

Observational signature.— The energy-momentum tensor for ϕ at late times is dominated by the contribution from the supercurvature mode. The spatial derivative term in $\langle T_{\mu\nu} \rangle$ gives a non-zero contribution, $\langle (\nabla\phi)^2 \rangle = -\langle \phi \nabla^2 \phi \rangle \sim 2\epsilon \langle \phi^2 \rangle$. If $\epsilon \ll 1$ and $m_0 \ll H_0$ (though these inequalities do not have to be very strong, in practice), the time-derivative term is negligible [1]. Then, the EoS parameter w_{DE} can be obtained by simply taking the ratio of p to ρ , and becomes

$$w_{\text{DE}} = -\frac{\frac{2}{3}(\epsilon/R_c^2) + m_0^2 a^2}{2(\epsilon/R_c^2) + m_0^2 a^2} = -\frac{1 + \frac{2}{3}\tilde{\epsilon}(1+z)^2}{1 + 2\tilde{\epsilon}(1+z)^2}. \quad (3)$$

where R_c is the comoving radius of curvature, which is constant⁶. The final expression shows that the functional form of $w_{\text{DE}}(z)$ depends on a single parameter⁷,

$$\tilde{\epsilon} \equiv \frac{\epsilon}{(m_0/H_0)^2} \Omega_{\text{K},0} \equiv \xi \Omega_{\text{K},0}, \quad (4)$$

where $\Omega_{\text{K},0} = 1/H_0^2 R_c^2$ is the fractional energy density of the spatial curvature at present. At late times, the mass term is dominant in (3), thus $w_{\text{DE}}(z) \rightarrow -1$. At

² The tunneling field does not have a supercurvature mode [12] which will give the residual effect at late times (as explained below), and cannot serve as a source for dark energy. Gravitons [13] and vector fields [14] also do not have one.

³ Extremely small mass $m_0 \sim H_0$ is considered to be possible because mass of a string axion arises typically due to instanton effects, and is exponentially sensitive to the instanton action [16].

⁴ For studies of the CMB in this framework, see e.g. [12, 17–20].

⁵ The dependence on the bubble size is not very strong: $c_\epsilon = 1/3$ in the small bubble limit, and $c_\epsilon = 2/9$ when the bubble occupies half of the ancestor de Sitter space.

⁶ The convention in [1] was to take $R_c = 1$. Here we take the scale factor at present to be 1, $a_0 = 1$, so that $a = 1/(1+z)$.

⁷ This corresponds to the $p = 2$, $w_0 = -1$, $w_1 = -1/3$ case in [25] (referred to “parametrization II” in [10]).

early times⁸, the spatial derivative term becomes dominant, thus $w_{\text{DE}}(z) \rightarrow -1/3$. The past asymptotic value $w_{\text{DE}}(z) \rightarrow -1/3$ is unlikely to be realized in the ordinary inflation: $\langle T_{\mu\nu} \rangle$ in de Sitter space with a de Sitter invariant vacuum should have $w = -1$; evolution of wave functions after inflation will give rise to non-zero time derivatives, not only spatial derivatives.

We regard the functional form of $w_{\text{DE}}(z)$ in (3) to be an indication of fluctuations generated before ordinary inflation⁹, but in fact, this may not be specific to open universe or bubble nucleation. If an infrared part of the fluctuations is enhanced relative to the usual magnitude H_I and is frozen until now, it will contribute to the spatial-derivative and mass terms of the energy-momentum tensor, giving the EoS parameter similar to (3). This can happen e.g., in a double inflation model in [26, 27].

Eq. (3) leads to a simple relation between w_0 and its derivative $w_a = -dw/da|_{a=1}$: When $\tilde{\epsilon} \ll 1$, we have $w_a = 2(w_0 + 1) = 8\tilde{\epsilon}/3$. This relation could be testable by ongoing observations such as Dark Energy Survey [28]. This will be a first step toward testing our model.

Eq. (3) yields the energy density of dark energy as a function of the redshift,

$$\rho_{\text{DE}}(z) = 3M_P^2 H_0^2 \Omega_{\Lambda,0} (1 + 2\tilde{\epsilon}(1+z)^2). \quad (5)$$

The mass term in the energy-momentum tensor gives the time-independent contribution $3M_P^2 H_0^2 \Omega_{\Lambda,0}$ to (5). The spatial derivative term gives a contribution with the relative factor $2\tilde{\epsilon}(1+z)^2$. In terms of the model parameters, $\Omega_{\Lambda,0}$ is given by¹⁰

$$\Omega_{\Lambda,0} = \frac{1}{6} \tilde{c}_* \frac{H_A^4}{H_0^2 M_P^2} \left(\frac{m_0}{m_A} \right)^2, \quad (6)$$

with $\tilde{c}_* = c_*(H_I/H_A)^{2\epsilon}$, where c_* depends on the size of the critical bubble¹¹ [1]. We can take $(H_I/H_A)^{2\epsilon} \sim 1$ when ϵ is sufficiently small. The parameters H_A , m_A , m_0 in the model are related to the observables, $\Omega_{\Lambda,0}$ and ξ as

$$\frac{H_A}{M_P} = \sqrt{\frac{6\xi\Omega_{\Lambda,0}}{\tilde{c}_*c_\epsilon}}, \quad \frac{m_A}{M_P} = \sqrt{\frac{6\Omega_{\Lambda,0}}{\tilde{c}_*}} \frac{\xi}{c_\epsilon} \frac{m_0}{H_0}. \quad (7)$$

We will forecast the constraints for ξ , rather than $\tilde{\epsilon} = \xi\Omega_{K,0}$. Since the definition of ξ is independent of $\Omega_{K,0}$, it

is not constrained to be very small; we expect $\xi = \mathcal{O}(1)$ as a natural choice. If we can determine ξ from observations, (7) allows us to determine an important parameter H_A .

Fisher analysis for galaxy surveys.— SKA [8] is a ground based array of radio telescopes which covers about 3/4 of the sky and observes galaxies by detecting the 21cm emission line of neutral hydrogen. Euclid [9] is a satellite based telescope working in the visible and near-infrared wavelength domains. SKA phase 2 (SKA2) and Euclid are both expected to observe a billion galaxies up to the redshift $z \sim 2$. In our analysis, we use the survey specifications described in [29] for SKA, and in [30] for Euclid. We take the power spectrum of galaxy distribution as an observable, and forecast the constraints on the parameters, following the standard procedure (see e.g., [32, 33, 35, 36]).

As the fiducial cosmological model, we take a w CDM model whose dark energy is characterized by w in (3) with the negative spatial curvature. The Hubble parameter $H(z)$ obeys

$$\frac{H^2}{H_0^2} = \Omega_{m,0}(1+z)^3 + \tilde{\Omega}_{K,0}(1+z)^2 + \Omega_{\Lambda,0}, \quad (8)$$

$$\frac{\dot{H}}{H^2} = -\frac{3}{2}\Omega_{m,0}(1+z)^3 - \tilde{\Omega}_{K,0}(1+z)^2. \quad (9)$$

Interestingly, the spatial derivative term in the energy-momentum tensor contributes exactly in the same way as the spatial curvature to Eqs. (8) and (9), effectively replacing $\Omega_{K,0}$ with $\tilde{\Omega}_{K,0} \equiv (1 + 2\xi\Omega_{\Lambda,0})\Omega_{K,0}$. Thus there is a tendency for degeneracy between $\Omega_{K,0}$ and ξ . On the other hand, the angular diameter distance, $D_A(z) = ((1+z)H_0\sqrt{\Omega_{K,0}})^{-1} \sinh(H_0\sqrt{\Omega_{K,0}} \int_0^z H^{-1}(z')dz')$, is defined in terms of the true curvature $\Omega_{K,0}$. This fact is expected to break the degeneracy.

We consider a model for galaxy distribution in the linear regime. The matter density contrast δ_m satisfies the k -independent equation at the linear level (see e.g., [37]),

$$\ddot{\delta}_m + 2H\dot{\delta}_m - \frac{3}{2}H^2\Omega_m\delta_m = 0. \quad (10)$$

An object of interest is the linear growth rate $f \equiv \frac{d \ln \delta_m}{d \ln a}$. The observed galaxy power spectrum in the redshift space is well described by

$$P_g(\mathbf{k}; z) = (b(z) + f(z)\mu^2)^2 P_m(k; z) e^{-k^2 \mu^2 \sigma_{\text{NL}}^2}, \quad (11)$$

where $P_m(k, z)$ is the linear matter power spectrum, and $b(z)$ is the so-called galaxy bias function, which should be chosen according to the type of target galaxies for the particular observation: for SKA, $b(z) = c_1 \exp(c_2 z)$ with constant c_1 and c_2 ; for Euclid, $b = \sqrt{1+z}$. The term $f\mu^2$, where μ is the cosine of the angle between the line of sight and the wave vector \mathbf{k} , represents the redshift space distortion [31], due to the contribution to the observed

⁸ Though we call it early times, we are assuming it to be later than the time when the supercurvature mode becomes dominant over the continuous modes.

⁹ Another possibility for realizing $w_{\text{DE}}(z)$ of (3) is to have two independent sources: one with $w = -1/3$ (such as cosmic strings) and the other with $w = -1$ (cosmological constant).

¹⁰ The fractional energy density of dark energy at present is the sum of the two terms, $\Omega_{\text{DE},0} = (1 + 2\tilde{\epsilon})\Omega_{\Lambda,0}$, but since $\tilde{\epsilon} \ll 1$, one can take $\Omega_{\text{DE},0} \approx \Omega_{\Lambda,0}$, in practice.

¹¹ We have $c_* = 3/8\pi^2$ in the small bubble limit, and $c_* = 3/4\pi^2$ when the bubble occupies half of the ancestor de Sitter space.

redshift from the peculiar velocity driven by the clustering of matter (making dense region look denser). The factor $e^{-k^2\mu^2\sigma_{\text{NL}}^2}$ with a free parameter $\sigma_{\text{NL}} \approx 7$ [Mpc] to be marginalized, is introduced to represent the inaccuracies in the observed redshift, which results in the line-of-sight smearing. Further, taking into account the geometrical effects due to the difference between the possibly incorrect reference cosmology and the true one, the so-called Alcock-Paczynski (AP) effect [34], the observed power spectrum is given by [33]

$$P_{\text{obs}}(\mathbf{k}_{\perp}^{\text{ref}}, k_{\parallel}^{\text{ref}}; z) = \left(\frac{D_{\text{A}}^{\text{ref}}(z)}{D_{\text{A}}(z)} \right)^2 \frac{H(z)}{H^{\text{ref}}(z)} P_{\text{g}}(\mathbf{k}_{\perp}, k_{\parallel}; z).$$

Here the angular diameter distance D_{A} and the Hubble parameter H in the reference cosmology are distinguished by the subscript ‘ref’, while those in true cosmology have no subscript. The wave number across and along the line-of-sight in the two cosmologies are related through $k_{\parallel} = \frac{H}{H^{\text{ref}}} k_{\parallel}^{\text{ref}}$ and $\mathbf{k}_{\perp} = \frac{D_{\text{A}}^{\text{ref}}}{D_{\text{A}}} \mathbf{k}_{\perp}^{\text{ref}}$.

The forecast.— The Fisher matrix for a set of parameters $\{\theta^{\alpha}\}$ is defined as $F_{\alpha\beta} = \left\langle \frac{\partial}{\partial\theta^{\alpha}} \frac{\partial}{\partial\theta^{\beta}} \log \mathcal{L} \right\rangle$ where \mathcal{L} is the likelihood function when we regard $\{\theta^{\alpha}\}$ as probabilistic variables which depends on the data set. The matrix $F_{\alpha\beta}$ is the inverse of the covariance matrix, and the minimum 1σ error on θ_{α} is given by $\sqrt{(F^{-1})_{\alpha\alpha}}$ (no sum on α). In terms of galaxy power spectrum, the Fisher matrix can be written as [33, 35]

$$F_{\alpha\beta} = \sum_{z_i} \int_{k_{\text{min}}}^{k_{\text{max}}} \frac{d^3\mathbf{k}}{(2\pi)^3} V_{\text{eff}}(\mathbf{k}; z_i) \times \frac{\partial \ln P_{\text{obs}}(\mathbf{k}; z_i)}{\partial\theta^{\alpha}} \frac{\partial \ln P_{\text{obs}}(\mathbf{k}; z_i)}{\partial\theta^{\beta}}, \quad (12)$$

where the effective volume of the survey is given by

$$V_{\text{eff}}(\mathbf{k}; z_i) \approx \left(\frac{n_{\text{g}}(z_i) P_{\text{obs}}(\mathbf{k}; z_i)}{n_{\text{g}}(z_i) P_{\text{obs}}(\mathbf{k}; z_i) + 1} \right)^2 V_{\text{survey}}(z_i). \quad (13)$$

The survey volume is divided into bins with the width $\Delta z = 0.1$ in the redshift. Here $V_{\text{survey}}(z_i)$ is the comoving volume of the redshift slice centered at z_i . The minimum wavelength is $k_{\text{min}}(z_i) = 2\pi/V_{\text{survey}}^{1/3}(z_i)$. The maximal wavelength is taken to be the scale beyond which non-linearities become non-negligible. It is estimated as $k_{\text{max}}(z_i) = 0.14(1+z_i)^{2/(2+n_s)}$ [Mpc $^{-1}$].

Our forecast is performed for the parameter set: $\{h, \Omega_{\Lambda,0}, \Omega_{\text{K},0}, h^2\Omega_{\text{b},0}, \sigma_8, n_s, \sigma_{\text{NL}}, b(z_i)\}$ and $\{\xi\}$. The fiducial values are taken as $h = 0.67$, $h^2\Omega_{\text{b},0} = 0.0222$, $\Omega_{\Lambda,0} = 0.6817$, $\sigma_8 = 0.834$, $n_s = 0.962$, $\Omega_{\text{K},0} = 0.03$, and $\xi = 0.8$.

FIG. 2 shows the forecast 1σ and 2σ contour in the $(\Omega_{\text{K},0}, \xi)$ plane for SKA2 and Euclid. There is degeneracy between $\Omega_{\text{K},0}$ and ξ along the $\tilde{\Omega}_{\text{K},0} = \text{const.}$ direction, for the reason mentioned above. However, for this

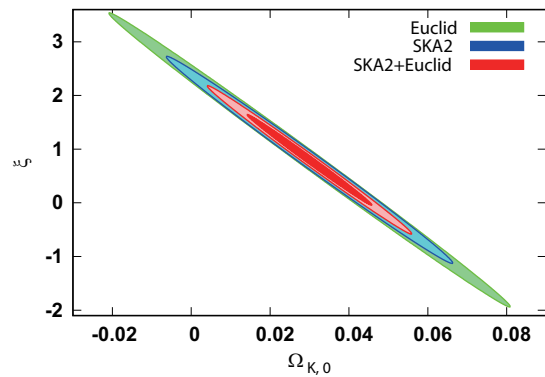


FIG. 2. Forecast 1σ and 2σ marginal contours with the fiducial values $(\Omega_{\text{K},0}, \xi) = (0.03, 0.8)$ for SKA2 galaxy survey (blue), Euclid (green), and the combined analysis (red).

set of fiducial values of the parameters, one can see the difference from $\xi = 0$ (i.e., time independent cosmological constant) at the 1σ level.

Discussion.— The above choice of parameters, $(\Omega_{\text{K},0}, \xi) = (0.03, 0.8)$, is barely consistent with the current constraint on the spatial curvature. These parameters may take smaller values. In that case, it might be difficult to determine these parameters solely from the results of galaxy surveys in the near future.

To break the degeneracy between $\Omega_{\text{K},0}$ and ξ , it is highly important to combine galaxy surveys with other observations of spatial curvature which have different dependence on the angular/luminosity/comoving distance. Possible detection of negative curvature by observations of the CMB will greatly improve the chance of determining the parameters, since the CMB involves larger z than the galaxy surveys, and will be more sensitive to the angular diameter distance. On the other hand, positive curvature at the level of $\Omega_{\text{K},0} \lesssim -10^{-4}$ would falsify bubble nucleation, as argued in [38], thus its detection would rule out our model.

If the results of galaxy surveys are consistent with our model with non-zero ξ , we may wonder whether this rules out other models. For instance, there is a quintessence model, called ‘‘scaling freezing’’ model¹², whose EoS parameter approaches $w_{\text{DE}} \rightarrow -1$ in the future and $w_{\text{DE}} \rightarrow 0$ in the past, and the transition occurs around $a \sim a_t$. Although it would be difficult for galaxy surveys at $z \lesssim 2$ to distinguish the past asymptotic values $w_{\text{DE}} \rightarrow -1/3$ and $w_{\text{DE}} \rightarrow 0$, in fact, there is already a strong constraint for the latter [39, 40]: The existing data of CMB, BAO, SNe, suggest that the transition has to occur quite early $a_t < 0.11$ (i.e., $z > 8.1$). Thus, the model with the past asymptotic behavior $w_{\text{DE}} \rightarrow 0$

¹² It is defined by the potential $V(\phi) = V_1 e^{-\lambda_1 \phi/M_P} + V_2 e^{-\lambda_2 \phi/M_P}$ where with $\lambda_1 \gg 1$ and $\lambda_2 \lesssim 1$. Its EoS parameter is well approximated by $w_{\text{DE}}(a) = -1 + 1/(1 + (a/a_t)^{1/\tau})$ with $\tau = 0.33$.

should have $w_{\text{DE}} \approx -1$ at $z \lesssim 2$, and cannot be responsible for the possible deviation from $w_{\text{DE}} = -1$ discussed in this Letter.

Acknowledgements.— We thank Jean-Baptiste Durrive for explaining their work [40]. YS would like to thank Lenny Susskind, Steve Shenker, Bob Wagoner, Adam Brown, Alex Maloney and Yusuke Yamada for comments at the seminar at Stanford Institute for Theoretical Physics. This work is supported in part by Grants-in-Aid for Scientific Research (Nos. 16K05329, 17K14304) from the Japan Society for the Promotion of Science. DSL and CPY are supported in part by the Ministry of Science and Technology, Taiwan.

* Email: yamauchi@jindai.jp

† Email: haoki@cc.saga-u.ac.jp

‡ Email: iso@post.kek.jp

§ Email: dslee@gms.ndhu.edu.tw

¶ Email: ysekino@la.takushoku-u.ac.jp

** Email: chenpinyeh@gmail.com

- [1] H. Aoki, S. Iso, D. S. Lee, Y. Sekino and C. P. Yeh, Phys. Rev. D **97**, no. 4, 043517 (2018) [arXiv:1710.09179 [hep-th]].
- [2] S. Perlmutter *et al.* [Supernova Cosmology Project Collaboration], Astrophys. J. **517**, 565 (1999) [astro-ph/9812133].
- [3] A. G. Riess *et al.* [Supernova Search Team], Astron. J. **116**, 1009 (1998) [astro-ph/9805201].
- [4] D. H. Weinberg, M. J. Mortonson, D. J. Eisenstein, C. Hirata, A. G. Riess and E. Rozo, Phys. Rept. **530**, 87 (2013) [arXiv:1201.2434 [astro-ph.CO]].
- [5] P. A. R. Ade *et al.* [Planck Collaboration], Astron. Astrophys. **594**, A13 (2016) [arXiv:1502.01589 [astro-ph.CO]].
- [6] P. A. R. Ade *et al.* [Planck Collaboration], Astron. Astrophys. **594**, A14 (2016) [arXiv:1502.01590 [astro-ph.CO]].
- [7] L. Amendola and S. Tsujikawa, “Dark Energy : Theory and Observations,” Cambridge University Press.
- [8] <https://www.skatelescope.org/>
- [9] <http://sci.esa.int/euclid/>
- [10] K. Kohri, Y. Oyama, T. Sekiguchi and T. Takahashi, JCAP **1702**, no. 02, 024 (2017) [arXiv:1608.01601 [astro-ph.CO]].
- [11] S. R. Coleman and F. De Luccia, Phys. Rev. D **21**, 3305 (1980).
- [12] J. Garriga, X. Montes, M. Sasaki and T. Tanaka, Nucl. Phys. B **551**, 317 (1999) [astro-ph/9811257].
- [13] T. Tanaka and M. Sasaki, Prog. Theor. Phys. **97**, 243 (1997) [astro-ph/9701053].
- [14] D. Yamauchi, T. Fujita and S. Mukohyama, JCAP **1403**, 031 (2014) [arXiv:1402.2784 [astro-ph.CO]].
- [15] B. Freivogel, M. Kleban, M. Rodriguez Martinez and L. Susskind, JHEP **0603**, 039 (2006) [hep-th/0505232].
- [16] A. Arvanitaki, S. Dimopoulos, S. Dubovsky, N. Kaloper and J. March-Russell, Phys. Rev. D **81**, 123530 (2010) [arXiv:0905.4720 [hep-th]].
- [17] A. D. Linde, M. Sasaki and T. Tanaka, Phys. Rev. D **59**, 123522 (1999) [astro-ph/9901135].
- [18] D. Yamauchi, A. Linde, A. Naruko, M. Sasaki and T. Tanaka, Phys. Rev. D **84**, 043513 (2011) [arXiv:1105.2674 [hep-th]].
- [19] K. Sugimura, D. Yamauchi and M. Sasaki, EPL **100**, no. 2, 29004 (2012) [arXiv:1208.3937 [astro-ph.CO]].
- [20] K. Sugimura, D. Yamauchi and M. Sasaki, JCAP **1201**, 027 (2012) [arXiv:1110.4773 [gr-qc]].
- [21] K. Yamamoto, M. Sasaki and T. Tanaka, Phys. Rev. D **54**, 5031 (1996) [astro-ph/9605103].
- [22] M. Sasaki, T. Tanaka and K. Yamamoto, Phys. Rev. D **51**, 2979 (1995) [gr-qc/9412025].
- [23] B. Freivogel, Y. Sekino, L. Susskind and C. P. Yeh, Phys. Rev. D **74**, 086003 (2006) [hep-th/0606204].
- [24] A. D. Linde, “Particle physics and inflationary cosmology,” CRC press, 1990 [hep-th/0503203].
- [25] S. Hannestad and E. Mortsell, JCAP **0409**, 001 (2004) [astro-ph/0407259].
- [26] H. Aoki, S. Iso and Y. Sekino, Phys. Rev. D **89**, no. 10, 103536 (2014) [arXiv:1402.6900 [hep-th]].
- [27] H. Aoki and S. Iso, PTEP **2015**, no. 11, 113E02 (2015) [arXiv:1411.5129 [gr-qc]].
- [28] <https://www.darkenergysurvey.org/>
- [29] S. Yahya, P. Bull, M. G. Santos, M. Silva, R. Maartens, P. Okouma and B. Bassett, Mon. Not. Roy. Astron. Soc. **450**, no. 3, 2251 (2015) [arXiv:1412.4700 [astro-ph.CO]].
- [30] L. Amendola *et al.*, Living Rev. Rel. **21**, no. 1, 2 (2018) [arXiv:1606.00180 [astro-ph.CO]].
- [31] N. Kaiser, Mon. Not. Roy. Astron. Soc. **227**, 1 (1987).
- [32] M. White, Y. S. Song and W. J. Percival, Mon. Not. Roy. Astron. Soc. **397**, 1348 (2008) [arXiv:0810.1518 [astro-ph]].
- [33] H. J. Seo and D. J. Eisenstein, Astrophys. J. **598**, 720 (2003) [astro-ph/0307460].
- [34] C. Alcock and B. Paczynski, Nature **281**, 358 (1979).
- [35] M. Tegmark, Phys. Rev. Lett. **79**, 3806 (1997) [astro-ph/9706198].
- [36] D. Yamauchi *et al.* [SKA-Japan Consortium Cosmology Science Working Group], PoS DSU **2015**, 004 (2016) [Publ. Astron. Soc. Jap. **68**, no. 6, R2 (2016)] [arXiv:1603.01959 [astro-ph.CO]].
- [37] P.J.E. Peebles, ‘Large Scale Structure of the Universe,’ Princeton University Press.
- [38] M. Kleban and M. Schillo, JCAP **1206**, 029 (2012) [arXiv:1202.5037 [astro-ph.CO]].
- [39] T. Chiba, A. De Felice and S. Tsujikawa, Phys. Rev. D **87**, no. 8, 083505 (2013) [arXiv:1210.3859 [astro-ph.CO]].
- [40] J. B. Durrive, J. Ooba, K. Ichiki and N. Sugiyama, Phys. Rev. D **97**, no. 4, 043503 (2018) [arXiv:1801.09446 [astro-ph.CO]].